Joint Detection of Multiple Orbital Angular Momentum Optical Modes

Mohammed Alfowzan, *Member, IEEE,* Jaime A. Anguita, *Member, IEEE* and Bane Vasic, *Fellow, IEEE,*

***Abstract*—We address the problem of detection in a multiple-beam orbital angular momentum (OAM)-based free-space optical communication link. Based on experimental channel observations, we extract a statistical model for the coaxial multimode OAM channel affected by atmospheric turbulence. We employ solutions to least square problems to compensate for the interference among optical modes. A solution based on Fincke-Pohst Enumeration Algorithm for least square problems is presented. In addition, Moore-Penrose based analytical solutions are considered (e.g. Zero Forcing). Finally, we provide bit error rate analysis for the channel under investigation.**

***Index Terms*—free-space optical communication; orbital angular momentum; turbulent channels; channel crosstalk.**

I. Introduction

FREE Space Optical (FSO) communications has been receiving increasing interest in providing high data rate communications. Especially at a time where conventional Radio Frequency (RF) systems are facing the challenge of bandwidth scarce resources in what is known as the spectrum gridlock [1]. Among different FSO signalling schemes Orbital Angular Momentum (OAM) is a viable contender in delivering very high speed point-to-point communications in a power efficient manner. OAM is a property of optical beams that can be exploited to allow the transmission of multiple data streams over different modes. These optical modes, also called optical vortices, do not interfere with each other. In other words, optical modes are mutually orthogonal. However, due to atmospheric turbulence and scintillation present in the terrestrial channel, orthogonality is no longer preserved which leads to interference between different optical vortices. The scintillation and cross talk between modes are captured in statistical models presented in [2] [3].

The effect of interference among modes can be depicted in a matrix representation that makes it natural to think of this as a least square problem as we will see later in this paper. One of this paper's important contributions is that a least square problem framework is presented to overcome cross talk between OAM optical modes. To the best of our knowledge, least square problem solutions have not been employed in the literature for the OAM cross talk channel. We will investigate the performance of the system using Moore-Penrose analytic solution, which is coined as the Zero Forcing (ZF) filter in the communication literature. The improved version known as the Minimum Mean Square Error (MMSE) filter that avoids noise enhancement is investigated.

In addition, we will employ reduced complexity enumeration techniques in finding solutions to least-square problems. These solutions are based on the Fincke-Pohst Enumeration Algorithm, also referred to as sphere decoding in the communication literature. The Fincke-Pohst Enumeration Algorithm gives near optimal solution with a reduced complexity relative to brute-force exhaustive search [4].

Evaluating the error rate performance is a quite involved problem for the OAM channel due to the intractability of the channel statistics and the interference. In this paper we relax the problem to make the analysis easer and we use the Moment Generator Function approach to derive the error rate. We will show that such relaxation of the problem yields good results for certain SNR regimes. Furthermore, we address the issue of optimal power assignment for the OAM channel under the separate detection scenario.

This paper is organized as follows. In section II the communication system architecture is presented. Also, the modulation formates of interest in this paper are discussed with a brief overview of their error rate performance over the Additive White Gaussian Noise (AWGN) channel which will used later in the error rate analysis over the OAM channel. Section III presents the channel statistical model and baseband channel model. In section IV the detection problem is addressed. We first consider the separate detection scenario where we provide error rate analysis of the OAM scintillation channel. Then, we present the joint detection approach which is based on the least square problem framework. For both detection approaches two modulation families are considered, namely amplitude based modulation (e.g. OOK) and position based modulation (i.e. PPM). We end this paper with concluding remarks in section V.

II. System Model

A. System Architecture

This section provides a general description of the system's main building blocks. Figure 1 depicts the communication architecture used in our OAM system. The top portion of the diagram represents the transmitter lineup. A binary source generates a sequence of length k $(b_i)_{i=1}^{k}$. In our system the bits are i.i.d. Bernoulli distributed. The mapper $\mathcal{M} : \{0,1\}^p \mapsto x_i$ is a bijection that takes upon a binary $p-tuple$ and maps it to a symbol. The symbol x_i is an element in the modulation

M. Alfowzan and B. Vasic are with the Department of Electrical and Computer Engineering, University of Arizona, AZ. Email:{alfowzan,vasic}@email.arizona.edu. M. Alfowzan is also affiliated with KACST.

J. A. Anguita is with the College of Engineering and Applied Sciences, Universidad de los Andes, Santiago, Chile. E-mail: janguita@miuandes.cl

This work is partially supported by NSF under Grant CCF-0963726 and Conicyt Chile, under grant Fondecyt-1120971.

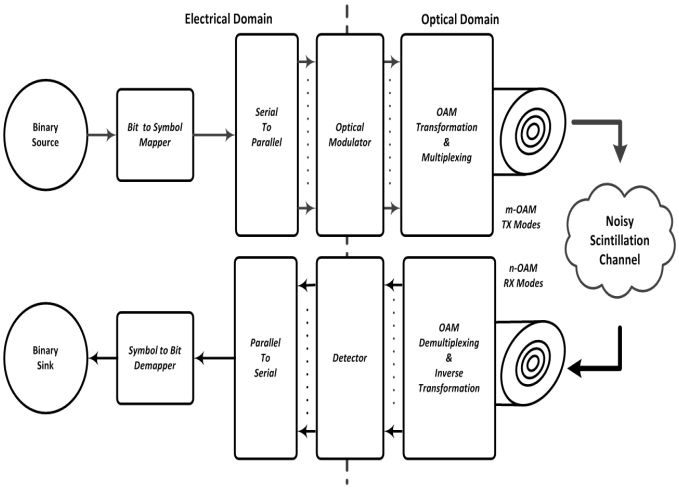

Fig. 1: Orbital Angular Momentum Based Communication System Architecture.

alphabet $\mathcal{X}$, of size $|\mathcal{X}| = 2^p$. The sequence of symbols $(x_i)_{i=1}^{l}$, where $l = \frac{k}{p}$, are then sent to the serial to parallel converter.

The serial to parallel converter takes a set of serial symbols $\{x_i, x_{i+1}, ..., x_{i+m}\}$, where m is the number of transmitted modes, and sends them in parallel fashion to an optical modulator. The optical modulator takes each symbol in $\{x_i, x_{i+1}, ..., x_{i+m}\}$ and emits light with intensity proportional to symbol electrical current (or voltage). Thus, this module converts the electrical signal to optical signal. More information on this will be given in the baseband model.

In the optical domain, two OAM operations are performed. The first one is multiplexing of light, where m light sources are multiplexed into a single OAM light beam with each light source assigned to a different optical mode. After that, an OAM transformation is performed, where different light modes are made collinear. Note that this setup allows the transmission of all channels through a single optical aperture (or optical antenna), thus reducing the size and weight of the system.

The receiver part of the system architecture performs the inverse operations of the transmitter described above. However, we want to highlight the most important part of the receiver, which is the detector block. The detector block in this paper performers two operations. In the first, the detector takes n optical streams and converts them to n electrical signals with currents proportional to the received optical intensity. In the second, the detector takes the n electrical signals and performs one of two types of detection approaches in this paper. In one approach all received signals are detected jointly as a vector (or array). We call this joint detection. In the other approach, each signal among the n signals is detected individually. We denote this as separate detection. This will be further explained in subsequent sections.

B. Description of the Modulation Formats

The modulation formats considered in this paper are based on the pervasive Intensity Modulation Direct Detection (IM-DD) signaling. Under such constraint no phase information can be obtained. Our primary modulation scheme is amplitude based. The transmitted symbol x_i is drawn from

$$\mathcal{X} = \{qd_{min} : q \in \mathbb{Z}_{\mathrm{Q}}\} \tag{1}$$

where, $\mathbb{Z}_{\mathrm{Q}} = \{0, 1, ..., Q-1\}$ and d_{min} is the distance separating two neighboring constellation points. Note that $Q = 2^p$. Given that the probability of error for and inner constellation point x_i point is $P_r\{|y - x_i| > \frac{dmin}{2}\}$, it not very hard to reach the symbol error probability

$$P_e = \frac{2(Q-1)}{Q}\mathrm{Q}\left(\sqrt{\frac{d_{min}^2}{N_o}}\right) \tag{2}$$

For the special case of On-Off keying (OOK), we get the error rate

$$P_e = \mathrm{Q}\left(\sqrt{\frac{d_{min}^2}{2N_o}}\right) = \mathrm{Q}\left(\sqrt{\frac{E_s}{2N_o}}\right) \tag{3}$$

For binary Pulse Position Modulation(PPM), it follows from the fact that its a two dimensional orthogonal modulation, thus the symbol and bit error probability is

$$P_e = \mathrm{Q}\left(\sqrt{\frac{d_{min}^2}{2N_o}}\right) = \mathrm{Q}\left(\sqrt{\frac{E_s}{N_o}}\right) \tag{4}$$

This error probability information over AWGN channel will be used later to evaluate the error rate for the OAM channel.

III. Channel Model

Orbital Angular Momentum can be achieved in different ways. Nonetheless, Laguerre-Gauss (LG) has been widely used due to its simplicity. The optical field distribution is given by

$$\begin{aligned} u_m(r,\phi,z) = &\sqrt{\frac{2p!}{\pi(p+|m|)!}}\ \frac{1}{\omega(z)}\ [\frac{r\sqrt{2}}{\omega(z)}]^{|m|} \\ &\times L_p^m[\frac{2r^2}{\omega^2(z)}]\ \exp[\frac{-r^2}{\omega^2(z)}]\ \exp[\frac{-ikr^2z}{2(z^2+z_R^2)}] \\ &\times \exp[i(2p+|m|+1)\ tan^{-1}(\frac{z}{z_R})]\ \exp[-im\phi] \end{aligned} \tag{5}$$

using the cylindrical coordinates, r and z are the radial and propagation distances, respectively. The azimuth angle is ϕ. The beam radius at distance z is $w(z) = w_o\sqrt{1+(\frac{z}{z_R})^2}$, where w_o is the radius of the zero-order gaussian beam at the waist. Rayleigh distance is $z_R = \frac{\pi w_o^2}{\lambda}$ and λ is the optical wavelength. The propagation constant is $k = \frac{2\pi}{\lambda}$. The generalized Laguerre polynomial is L_p^m with p being the radial and m the angular mode number.

For a pair of LG modes $u_i(r,\phi,z)$ and $u_j(r,\phi,z)$, where

$i \neq j$, the two mode are known to be orthogonal. To be explicit

$$\begin{aligned} &< u_i(r,\phi,z), u_j(r,\phi,z) > \\ &\triangleq \int\int u_i(r,\phi,z) u_j^*(r,\phi,z)\ r dr d\phi \\ &= \begin{cases} 0, & i \neq j; \\ \int\ u_i(r,\phi,z) r dr d\phi, & \text{otherwise}, \end{cases} \end{aligned} \tag{6}$$

However, due to imperfections of the channel caused by the atmospheric turbulence, the orthogonality does not always hold (i.e. $< u_i(r,\phi,z), u_j(r,\phi,z) > \neq 0,$ for $i \neq j$).

A. Baseband Channel Model

After this brief overview of the OAM beam, we will present the baseband model which will be the basis of our analysis. The following equation depicts the real-valued baseband signal transmitted over i^{th} mode

$$I_i(t) = g_i x_i(t) |u_i(r,\phi,z)|^2 \tag{7}$$

where g_i is the laser gain of the i^{th} mode with the units of $W/(A \cdot m^2)$. The transmitted signal is $x_i(t)$ over the i^{th} mode and $u_i(r,\phi,z)$ is the Gauss-Laguerre field for the given parameters. Note that in optical systems its not common to put emphasis on the passband model (i.e. $I_i(t) = g_i x_i(t) |u_i(r,\phi,z)|^2 \cos(2\pi f_c t)$) since at optical frequency f_c its extremely difficult to capture frequency information. It follows that the received signal is

$$y_i(t) = r_i g_i x_i(t) * h_{ii}(t) + \sum_{j \neq i} r_j g_j x_j(t) * h_{ij}(t) + n_i(t) \tag{8}$$

where r_i is the receiver sensitivity with units of $(A \cdot m^2)/W$. The channel impulse response from the j^{th} transmission mode to the i^{th} receiving mode is $h_{ij}(t)$. The operator $*$ represents convolution. The second term is the sum of the cross-talk between different modes due to atmospheric turbulence. The additive gaussian noise with mean zero and variance σ_n is $n_i(t)$. For simplicity of analysis, laser gain and receiver sensitivity are assumed to have unity value (i.e. $r_i = 1$ and $g_i = 1,\ \forall\ i$). In addition, we consider the discrete time model by suppressing the time index

$$y_i = x_i h_{ii} + \sum_{j \neq i} x_j h_{ij} + n_i \tag{9}$$

From (9) arises the matrix representation of the problem $\mathbf{y} = \mathbf{Hx} + \mathbf{n}$. This matrix representation will be considered in following sections.

B. Statistical Description of the Channel

This section provides the statistical description of the OAM scintillation channel over the desired mode (h_{ij}, for $i = j$) and the statistical description of interfering OAM modes (h_{ij}, for $i \neq j$). In this paper we will only consider the weak atmospheric turbulence case. All statistics are obtained from an optical propagation model run for thousands of channel instances with a method that is widely accepted [2]. From the obtained fading histograms, it has been found that in the weak atmospheric turbulence regime, the Johnson S_B distribution is the best fit for the desired channel scintillation [3]. Its density is given by

$$fy(y|\gamma,\delta) = \frac{\delta}{\sqrt{2\pi}} \frac{1}{y(1-y)} \exp\left\{\frac{1}{2}\left[\gamma + \delta \frac{y}{1-y}\right]\right\} \tag{10}$$

where the distribution parameters are γ and δ. It has been also found that the interfering signals are exponentially distributed with mean $\frac{1}{\lambda}$. Table I and II summarize the statistical distribution for the interfering and desired signals. Going back to the matrix representation $\mathbf{y} = \mathbf{Hx} + \mathbf{n}$, notice that the diagonal elements of H will be S_B Johnson distributed and the off diagonal elements will be exponentially distributed with the corresponding parameters.

TABLE I: Desired Signal Distribution

	Weak Turbulence	
Distribution	Parameters	
Johnson S_B	$\gamma = -2.7$	$\delta = 1.004$

TABLE II: Interference Signal Distribution

Weak Turbulence			
Neighbor	Distribution	Parameters	
First	*Exponential*	$\frac{1}{\lambda} =$	0.044
Second	*Exponential*	$\frac{1}{\lambda} =$	5×10^{-3}
Third	*Exponential*	$\frac{1}{\lambda} =$	1.04×10^{-3}

IV. Detection Strategies

A. Separate Detection and Bit Error Rate Analysis

In this section we consider the case of separate detection. We have discussed that under weak atmospheric turbulence the distribution of intended channel is S_B Johnson and the interfering signals have exponential distribution. For ease of analysis we relax the problem and we model the interference as part of the added gaussian noise with variance proportional to interference level ($i.e.\ n_{\text{total}} = n_{\text{interference}} + n_{\text{awgn}}$) yielding

$$y_i = s_i\ h_i + n_{total} \tag{11}$$

However, the S_B Johnson distribution that models the intended channel scintillations is analytically intractable. Thus, we resort to using the Nakagami-m distribution to model intended channel scintillations. We stress that this is only done in our analytical work, however the simulations are still performed using channel statistics presented previously. The SNR will then be Gamma distributed. Therefore, the symbol error rate of this scintillation channel is

$$\bar{P}_{sc} = \int_0^\infty P_e(\gamma)\ f_\gamma(\gamma) d\gamma. \tag{12}$$

Using the alternative Q-function representation

$$Q(x) = \frac{1}{\pi} \int_0^{\pi/2} exp[\frac{-x^2}{2\ sin^2\ \phi}]\ d\phi, x > 0 \tag{13}$$

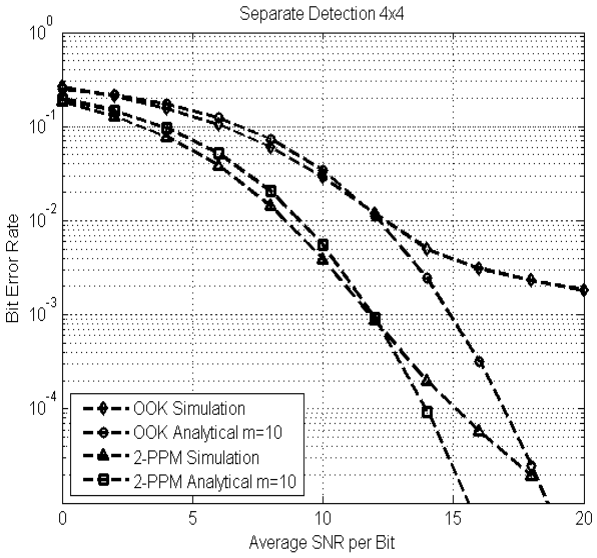

Fig. 2: BER for Separate Detection simulation and analytical results.

Applying the Moment-Generating function approach for evaluating symbol error rates

$$\bar{P}_{sc} = \frac{1}{\pi}\int_0^{\infty}\int_0^{\pi/2} exp[-c\frac{\gamma}{sin^2\ \phi}]\ d\phi\ f_{\gamma}\ (\gamma)d\gamma \tag{14}$$

$$\bar{P}_{sc} = \frac{1}{\pi}\int_0^{\pi/2} \Phi(\frac{-c}{sin^2\phi})\ d\phi \tag{15}$$

Using the Gamma distribution Moment generating function $\Phi(.)$ we get

$$\bar{P}_{sc} = \frac{1}{\pi}(1+c\frac{\gamma}{m})^{-m} \tag{16}$$

From (3) it is easy to see that for the OOK modulation we get the following error probability

$$\bar{P}_{sc} = \frac{1}{\pi}(1+\frac{1}{4m}\frac{E_s}{N_o})^{-m} \tag{17}$$

Similarly from (4) for PPM we arrive at

$$\bar{P}_{sc} = \frac{1}{\pi}(1+\frac{1}{2m}\frac{E_s}{N_o})^{-m} \tag{18}$$

Figure 2 shows the error rate curves for two modulation formats both simulated and analytical. For the OOK case we see that our analytical result matches the simulated result for the low to moderate SNR regime. Beyond that ($\sim$ 12.5dB) the two curves diverge. The reason is that the interference from other modes start dominating the error performance and we see that the BER curve hits an error floor. Similar comment can be made about PPM. Due to the bad performance of separate detection and the very high error floor that it suffers we employ different detection techniques as we will see in the following two sections.

Before we move to the joint detection section we briefly address the issue of optimal power assignment over different modes. From (9) we can see that the SINR for mode i takes the following form

$$\text{SINR}_i = \frac{P_i h_{ii}^2}{\sum\limits_{\substack{\forall j \\ j\neq i}} P_j h_{ij}^2 + N_o} \tag{19}$$

hence the achievable rate is

$$\mathcal{R}_i = \log_2(1+\frac{P_i h_{ii}^2}{\sum\limits_{\substack{\forall j \\ j\neq i}} P_j h_{ij}^2 + N_o}) \tag{20}$$

Therefore, it is clear that this is an optimization problem with set $\mathcal{P} = \{P_1, \ldots, P_m\}$ being the decision variables to maximize the sum rate $\Sigma_{\forall i} R_i$ as

$$\begin{aligned} &\max_{\mathcal{P}} \sum_{\forall i} \mathcal{R}_i \\ &\text{s.t.} \sum_{\forall i} P_i \preceq P_{max} \\ &\mathcal{P} \succeq 0 \end{aligned} \tag{21}$$

The first constraint insures that the sum of assigned powers does not exceed a maximum value P_{max}. The second constraints the assigned powers not to take on negative values.

B. Joint Detection

In this section we will consider detecting OAM mode jointly. Two approaches are investigated *i*) Moore–Penrose based Detection *ii*) Fincke-Pohst Enumeration algorithm based detection. For both approaches we consider two modulation scenarios a) amplitude based modulation (e.g. OOK) b) position based modulation (i.e. PPM).

*1) **Moore–Penrose Based Detection**:*

*a) **Amplitude Based Modulation**:* Consider the problem $b = Ax$, where $b \in \mathcal{R}^n$, $A \in \mathcal{R}^{n\times m}$ and $x \in \mathcal{R}^m$. For such a problem there exists an analytical solution by using Moore–Penrose pseudo inverse $A^{\dagger} = (A^T A)^{-1}A^T$. It has been shown that multiplying both sides of $b = Ax$ yields a solution $\hat{x}$ such that it gives the minimum mean square error value $||b - A\hat{x}||^2$. This solution is widely adopted in the communication literature, and its usually referred to as the Zero-Forcing. In our system if we have a channel matrix $H \in R^{n\times m}$ the zero forcing filter is given by

$$\mathbf{G}_{\text{ZF}} = \mathbf{H}^{\dagger} = (\mathbf{H}^H\mathbf{H})^{-1}\mathbf{H}^H. \tag{22}$$

Therefore, for the received vector $\mathbf{y}$ we detect $\mathbf{x}$ by applying the ZF filter

$$\begin{aligned} \hat{\mathbf{x}} = \mathbf{G}_{\text{ZF}}\mathbf{y} &= (\mathbf{H}^H\mathbf{H})^{-1}\mathbf{H}^H\mathbf{H}\mathbf{x} + (\mathbf{H}^H\mathbf{H})^{-1}\mathbf{H}^H\mathbf{n} \\ &= \mathbf{x} + (\mathbf{H}^H\mathbf{H})^{-1}\mathbf{H}^H\mathbf{n} = \mathbf{x} + \mathbf{H}^{\dagger}\mathbf{n} \end{aligned} \tag{23}$$

however, as we can see form the right hand side of (23) that applying this filter will cause noise enhancement $H^{\dagger}n$. Thus the MMSE filter is used to overcome this problem

$$\mathbf{G}_{\text{MMSE}} = (\mathbf{H}^H\mathbf{H} + \frac{\sigma_n^2}{\sigma_x^2}I)^{-1}\mathbf{H}^H = (\mathbf{H}^H\mathbf{H} + \frac{1}{\text{SNR}}I)^{-1}\mathbf{H}^H \tag{24}$$

*b) **Pulse Position Based Modulation**:* For a general Q-ary Pulse Position Modulation (Q-PPM) the system can be

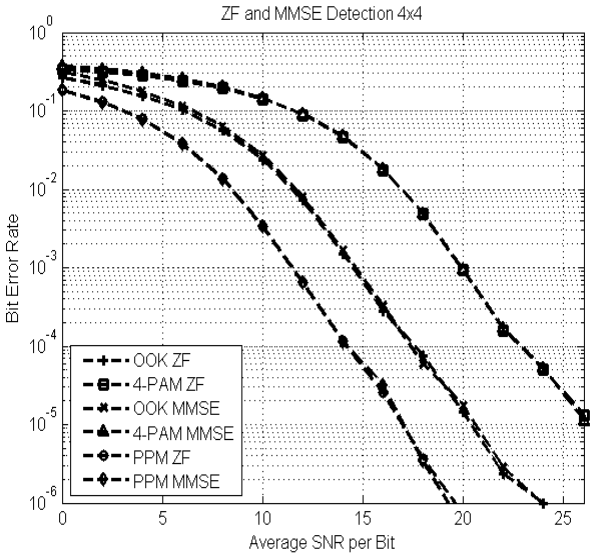

Fig. 3: BER for ZF and MMSE based Detection.

represented as

$$\begin{bmatrix} \mathbf{y}_1 \\ \vdots \\ \mathbf{y}_Q \end{bmatrix} = \begin{bmatrix} \mathbf{H}_1 & \cdots & 0 \\ \vdots & \ddots & \vdots \\ 0 & \cdots & \mathbf{H}_Q \end{bmatrix} \begin{bmatrix} \mathbf{x}_1 \\ \vdots \\ \mathbf{x}_Q \end{bmatrix} + \begin{bmatrix} \mathbf{n}_1 \\ \vdots \\ \mathbf{n}_Q \end{bmatrix} \tag{25}$$

where $\mathbf{y}_i$ and $\mathbf{x}_i$ are the received pulses vector and the transmitted pulses vector in the i^{th} time slot respectively. The channel matrix for the i^{th} time slot is $\mathbf{H}_i$. We will assume that $\mathbf{H}_i$ for all $i \in \{1, .., Q\}$ are the same. Also, $\mathbf{n}_i$ is the noise vector for the corresponding time slot. Due to the time orthogonality the system can be decomposed to subsystems which reduces the complexity as follows

$$\mathbf{y}_1 = \mathbf{H}\mathbf{x}_1 + \mathbf{n}_1, \ \cdots, \ \mathbf{y}_Q = \mathbf{H}\mathbf{x}_Q + \mathbf{n}_Q \tag{26}$$

We can apply $H^\dagger$ to $\{\mathbf{y}_1, \ \cdots, \ \mathbf{y}_Q\}$ to find $\{\hat{\mathbf{x}}_1, \ \cdots, \ \hat{\mathbf{x}}_Q\}$ and thus we can demodulate.

The error rate performance for the MMSE and ZF detection is shown in Figure 3. The important thing to notice is that there is no noticeable gain achieved by MMSE over ZF. The reason is that statistics of this channel, where the diagonal elements are dominant and the off diagonal elements are much smaller. It is expected that for the moderate and strong turbulence case we will notice an improvement by using MMSE over ZF. Comparing Figure 3 and 2 it is also important to notice that ZF and MMSE outperform the separate detection approach.

*2) **Fincke-Pohst Enumeration Algorithm**:*

*a) **Amplitude Based Modulation**:*

$$\mathbf{y} = \mathbf{H}\mathbf{x} + \mathbf{n} \tag{27}$$

Consider the linear system in (27) with $H \in R^{n \times m}$, $x \in Z^m$, $y \in R^n$ and $n \in R^n$. It is not difficult to see that this problem is a least square problem with the optimal solution

$$\hat{\mathbf{x}} = \underset{x \in \mathcal{X}^m}{\arg\min} \ ||\mathbf{y} - \mathbf{H}\mathbf{x}||^2, \tag{28}$$

this solution is optimal in the sense that the ML detector f that maps the channel output $f : y \to \hat{x}$, minimizes the error probability P_e. This optimality comes at the expense of complexity due to the exhaustive search process. However Fincke-Pohst Enumeration Algorithm (a.k.a. sphere decoder in the communications literature) only considers the lattice points within a sphere of radius d

$$d^2 \geq ||\mathbf{y} - \mathbf{H}\mathbf{x}||^2. \tag{29}$$

Using QR factorization, the channel matrix can be represented as

$$\mathbf{H} = [\mathbf{Q}_1 \ \mathbf{Q}_2] \begin{bmatrix} \mathbf{R} \\ \mathbf{0} \end{bmatrix}. \tag{30}$$

such that

$$\mathbf{y} = [\mathbf{Q}_1 \ \mathbf{Q}_2] \begin{bmatrix} \mathbf{R} \\ \mathbf{0} \end{bmatrix} \mathbf{x} + \mathbf{n} \tag{31}$$

For this slightly altered representation, the analog of equation (29) is

$$||\mathbf{y} - [\mathbf{Q}_1 \ \mathbf{Q}_2] \begin{bmatrix} \mathbf{R} \\ \mathbf{0} \end{bmatrix} \mathbf{x}||^2 \leq d^2 \tag{32}$$

$$|| \begin{bmatrix} \mathbf{Q}_1^H \\ \mathbf{Q}_2^H \end{bmatrix} \mathbf{y} - \begin{bmatrix} \mathbf{R} \\ \mathbf{0} \end{bmatrix} \mathbf{x}||^2 \leq d^2 \tag{33}$$

where H in $\mathbf{Q}_1^H$ is the hermitian transpose

$$||\underbrace{\mathbf{Q}_1^H \mathbf{y}}_{\mathbf{z}} - \mathbf{R}\mathbf{x}||^2 \leq \underbrace{d^2 - ||\mathbf{Q}_2^H \mathbf{y}||}_{d'^2} \tag{34}$$

from the upper triangular relation in (34) it could be shown that

$$d'^2 \geq \Sigma_{i=1}^m (z_i - \Sigma_{j=i}^m r_{i,j} x_j)^2. \tag{35}$$

An important remark about the altered representation using QR factorization is that this representation introduces a recurrence relation where the detector starts with the symbol x_m and goes up until symbol x_1 is detected. More details can be found in [5] [4].

*b) **Pulse Position Based Modulation**:* Following the same line of reasoning in (26) and (25) our system can take the following form

$$||\mathbf{y}_1 - \mathbf{H}\mathbf{x}_1||^2 \leq d^2, \ \cdots, \ ||\mathbf{y}_Q - \mathbf{H}\mathbf{x}_Q||^2 \leq d^2 \tag{36}$$

Consider the case of 2-PPM. The possible values that it can take for the two time slots are $(1, 0)$ or $(0, 1)$. However, due to the nature of this detection approach where the outputs are integers and the fact that we decomposed our system its possible to detect $(1, 1)$ and $(0, 0)$, which is invalid. In this paper we will not consider a resolution mechanism to overcome this problem.

We can see in Figure 4 the BER curves for different modulations formats using Fincke-Pohst Enumeration based detection. It is not surprising that it offers superior performance over MMSE and ZF detection since the Fincke-Pohst Enumeration is a relaxed version of ML detection. The perhaps surprising result is that 2-PPM and OOK have the approximately the same performance. This degradation of performance for the PPM case is due to the decomposition

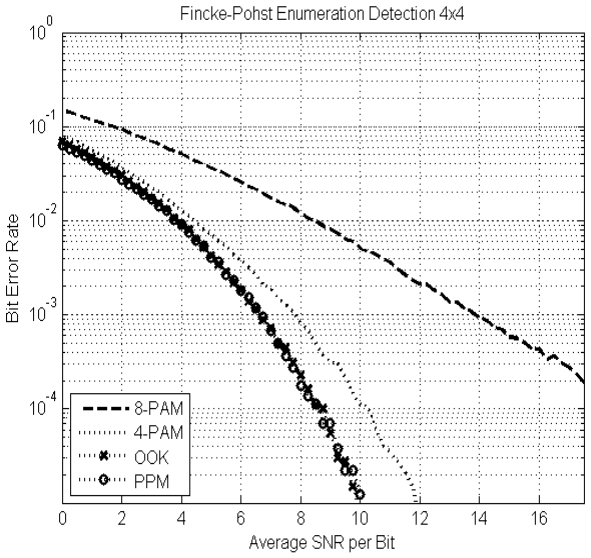

Fig. 4: BER for Fincke-Pohst Enumeration based Detection.

of the problem which reduces the complexity at the expense of performance. However, PPM for decomposed Fincke-Pohst Enumeration algorithm significantly out performs the Moore–Penrose based detection.

V. Conclusions

This paper addresses the problem of interference between optical modes in orbital angular momentum channels. We exploited statistical properties and the matrix representation of the OAM channel to use solutions of least square problems. These solution vary in terms of complexity and performance. Fincke-Pohst Enumeration Algorithm possess superior performance, however they are more complex than Moore-Penrose based solutions. Finally an error rate analysis was presented for separate detection case.

References

[1] Goldsmith, A.; Jafar, S.A.; Maric, I.; Srinivasa, S., "Breaking Spectrum Gridlock With Cognitive Radios: An Information Theoretic Perspective," Proceedings of the IEEE , vol.97, no.5, pp.894,914, May 2009

[2] Anguita, J.; Neifeld, M.; Vasic, B.,"Turbulence-induced channel crosstalk in an orbital angular momentum-multiplexed free-space optical link", Applied Optics ,Vol. 47, Issue 13, pp. 2414-2429 (2008)

[3] Jaime A. Anguita ; Joaquin Herreros; "Experimental analysis of orbital angular momentum-carrying beams in turbulence", Proc. SPIE 8162, Free-Space and Atmospheric Laser Communications XI, 816207 (September 14, 2011);

[4] Damen, M.-O.; El-Gamal, H.; Caire, G., "On maximum-likelihood detection and the search for the closest lattice point," Information Theory, IEEE Transactions on , vol.49, no.10, pp.2389,2402, Oct. 2003

[5] U. Fincke and M. Pohst, "Improved methods for calculating vectors of short length in a lattice, includ- ing a complexity analysis," Mathematics of Computation, vol. 44, pp. 463-471, April 1985.